Polymer Chemistry

PAPER

View Article Online
View Journal | View Issue

Cite this: *Polym. Chem.*, 2015, **6**, 3353

'Blocky' donor–acceptor polymers containing selenophene, benzodithiophene and thienothiophene for improved molecular ordering†

Dong Gao, Gregory L. Gibson, Jon Hollinger, Pengfei Li and Dwight S. Seferos*

Received 20th February 2015,
Accepted 19th March 2015

DOI: 10.1039/c5py00276a

www.rsc.org/polymers

Controlling the phase-separation behavior and achieving an ideal morphology has turned into one of the most important challenges in the field of polymer electronics. In this study we report a straightforward route to 'blocky' copolymers that incorporates selenophene into a benzodithiophene (BDT)–thienothiophene (TT) donor–acceptor system for improved molecular ordering. The blocky structure preserves the optical properties of the parent polymers, which is different than an analogue employing purely statistical sequence. Peak force quantitative nanomechanical mode atomic force microscopy reveals a more ordered network-like morphology in blocky polymer:$PC_{71}BM$ films. However the photovoltaic properties of blocky polymers are still lower than the physical mixtures of the two parent polymers. This blocky copolymer approach can be applied to many other polymerization methods to prepare many new types of blocky D–A polymers. As such, it could be a new tool for tuning the polymer crystallinity, and eventually achieving controllable solid-state morphology for polymer electronic applications.

Introduction

Donor–acceptor (D–A) conjugated polymers have been central to polymer photovoltaic research for the past two decades. Notable examples include poly[*N*-9′-heptadecanyl-2,7-carbazole-*alt*-5,5-(4′,7′-di-2-thienyl-2′,1′,3′-benzothiadiazole)] (PCDTBT),[1] poly[2,6-(4,4-bis-(2-ethylhexyl)-4*H*-cyclopenta [2,1-*b*:3,4-*b*′]dithiophene)-*alt*-4,7(2,1,3-benzothiadiazole)] (PCPDTBT)[2] and poly({4,8-bis[(2-ethylhexyl)oxy]benzo[1,2-*b*:4,5-*b*′]dithiophene-2,6-diyl}{3-fluoro-2-[(2-ethylhexyl)carbonyl]thieno[3,4-*b*]-thiophenediyl}) (PTB7),[3] which reach champion power conversion efficiencies of 7.2%,[4–6] 5.8%,[2] and 9.2%,[7] respectively. For all of the above materials the solubilizing side-chains were optimized to obtain the best photovoltaic performances. These examples are few in number relative to the vast reported structures that do not reach acceptable performance yet have 'ideal' or near ideal optical properties and HOMO–LUMO energy levels. While side-chain engineering has been the most important method for tuning the polymer solubility and solid-state properties, finding the optimal morphology is almost a trial-and-error process and requires major synthetic efforts. This is due to the extreme difficulty in predicting solid-state morphology. Controlling phase-separation with an electron acceptor and achieving an ideal morphology has indeed turned into one of the most important challenges in the field.

Crystalline polymer domains play an important role in improving charge separation, charge carrier mobility, and device stability.[8,9] However many D–A polymers have low crystallinity. For instance, Grazing Incidence Wide-angle X-ray Scattering (GIWAXS) analysis shows that poly[4,8-bis(5-(2-ethylhexyl)thiophen-2-yl)benzo[1,2-*b*:4,5-*b*′]dithiophene-2,6-diyl-*alt*-(4-(2-ethylhexanoyl)-thieno[3,4-*b*]thiophene-)-2-6-diyl)] (PBDTTT-C-T) has no clear π–π stacking reflection, highlighting the very low crystallinity of this polymer.[10] On the other hand, recent studies have showed introducing heavy atoms into the polymer backbone can increase the tendency of the polymer to form better ordered phases, leading better charge carrier mobility.[11–21] Doing so may also decrease the solubility and increase the difficulty of polymer purification and processing.[22,23] Therefore it would be interesting to develop polymers that contain a D–A structure with some incorporation of heavy atoms and ideally achieve a block-like sequence as a means to improve the molecular ordering of polymer.

In this study we report a straightforward route to blocky copolymers that incorporate selenophene into a benzodithiophene (BDT)-thienothiophene (TT) donor–acceptor system. Because the HOMO energy level of D–A polymer is mostly localized at donor moieties, substituting TT with selenophene retains the delocalization of HOMO level over the polymer.

Department of Chemistry, University of Toronto, 80 St. George Street, Toronto, Ontario M5S 3H6, Canada. E-mail: dseferos@chem.utoronto.ca

†Electronic supplementary information (ESI) available. See DOI: 10.1039/c5py00276a

Meanwhile, formation of blocks preserves the optical properties of the parent polymers, which is different to an analogue employing statistical sequence. The photovoltaic properties of blocky polymers are compared together with the statistical polymer and physical mixtures of the parent polymers, which give us a clearer idea of the phase-separation behavior of the blocky polymer in films that also contain fullerene-acceptors.

Polymer synthesis and characterization

The blocky polymers were synthesized through a three-step Stille coupling (Scheme 1). Briefly, donor–acceptor polymer fragments with trimethyltin or Br end-groups were prepared by using an excess of one of the monomer type (either di-halo or di-stanyl coupling partner) and then coupled together in a third polymerization. Polymer fragments incorporating selenophene (PBDTSe-T fragments) with trimethyltin end-groups were synthesized with a benzodithiophene (BDT) : selenophene monomer ratio of 1.2 : 1. After heating to reflux in toluene for 4 hours, the reaction mixture of PBDTSe-T fragments was precipitated into hexane and washed twice to remove excess monomer and low molecular weight fragments. Three complementary fragments incorporating thienothiophene (PBDTTT-C-T fragments) with Br end-groups were prepared with varied BDT: thienothiophene monomer ratios (1 : 1.1, 1 : 1.15 and 1 : 1.2 mol : mol), to produce PBDTTT-C-T fragments with different molecular weights. Each PBDTTT-C-T fragment product was precipitated into methanol, which also eroded any remaining trimethyltin end-groups. The precipitate was then placed in a Soxhlet apparatus and washed with hexanes and extracted with chloroform. Finally, a third polymerization was carried out with equal amounts (mol : mol) of PDBTSe-T and PDBTTT-C-T fragments. The ratio of selenophene and TT monomers in the three blocky polymers are 1 : 1.59, 1 : 1.16 and 1 : 0.85, based on molecular weights of their respective PBDTSe-T fragments and PBDTTT-C-T fragment reactants (Table 1). Two parent copolymers, poly[4,8-bis(5-(2-ethylhexyl)thiophen-2-yl)benzo-[1,2-*b*:4,5-*b*′]dithiophene-2,6-diyl-*alt*-selenophene] (PBDTSe-T) and poly[4,8-bis(5-(2-ethylhexyl)thiophen-2-yl)benzo[1,2-*b*:4,5-*b*′]dithiophene-2,6-diyl-*alt*-(4-(2-ethylhexanoyl)-thieno[3,4-*b*]-thiophene-)-2-6-diyl)] (PDBTTT-C-T)[24] and a statistical copolymer with a Se and TT monomer ratio of 1 : 1 (mol : mol) were also synthesized to complete the study.

Table 1 Summary of copolymer composition, number average molecular weight (M_n)[a], dispersity ($Đ$) and optical energy gap (E_g^{opt})[b] Se : TT stands for the ratio of the amount of selenophene monomers to the amount of thienothiophene monomers

Polymer	Se : TT (mol : mol)	M_n (kDa)	$Đ$	E_g^{opt} (eV)
1 : 1.59 blocky	1 : 1.59	20.9	3.0	1.54
1 : 1.16 blocky	1 : 1.16	22.1	2.7	1.54
1 : 0.85 blocky	1 : 0.85	17.7	2.8	1.54
1 : 1 statistical	1 : 1	19.2	2.2	1.59

[a] Calibrated with polystyrene standards using 1,2,4-trichlorobenzene as eluent at 140 °C. [b] Determined by the onset of film absorption spectrum.

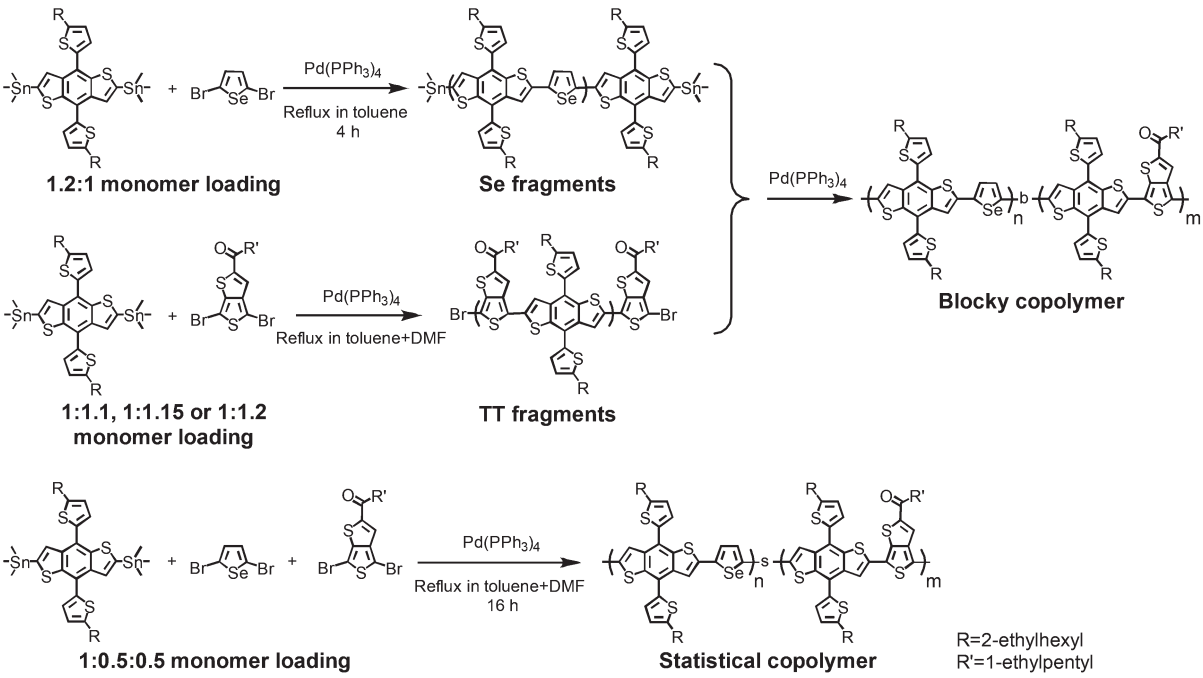

Scheme 1 Synthetic routes to blocky and statistical copolymers (R = 2-ethylhexyl, R′ = 1-ethylpentyl).

All blocky polymers incorporated PBDTSe-T fragment had a number average molecular weight (M_n) of 8.0 kDa. Molecular weights of PBDTTT-C-T fragments were 15.3 kDa, 10.9 kDa and 8.0 kDa, for blocky polymer with selenophene : thienothiophene monomer ratio (mol : mol) of 1 : 1.59, 1 : 1.16 and 1 : 0.85, respectively. Fragment coupling and formation of blocky polymers was confirmed by GPC analysis. After the third polymerizations a new elution peak was observed at smaller retention volume in all cases (Fig. 1 and S1,† Table 1). Polymer molecular weights are roughly doubled compared with fragment reactants, indicating most of polymers are di-block structures. However it is also clear from the GPC that a small amount of unreacted parent polymer or multi-blocks polymer is present. Therefore we use the term "blocky" to describe the structures of polymer studied here.

Absorption spectra were collected for both solutions (Fig. 2) and thin films (Fig. 3). The absorption profiles of blocky polymers have distinct peaks that correspond to the two parent structures. This is in contrast to the statistical copolymer, which only has one broad absorption band at a longer wavelength. Optical energy gaps were determined by the onset of thin film absorptions (Table 1). The optical properties of two parent structures are preserved in the blocky polymers.

The ordering of blocky and statistical polymers was first investigated with X-ray diffraction (Fig. S2 and S3†). The broad diffraction peak at $2\theta \sim 23.3°$ may come from SiO_2 contaminants on the Si wafer.[25] The blocky polymers also have a weak reflection at $2\theta \sim 4.5°$, corresponding to an interlayer spacing of ~20 Å. This peak is more obvious in polymer:$PC_{71}BM$ blend films due to the lower background signal. On the other hand the statistical polymer did not produce a clear interlayer spacing reflection. Interestingly, the 1 : 1.16 blocky polymer shows an additional signal at $2\theta \sim 3.2°$. This signal may come from different orientations of polymer backbones.

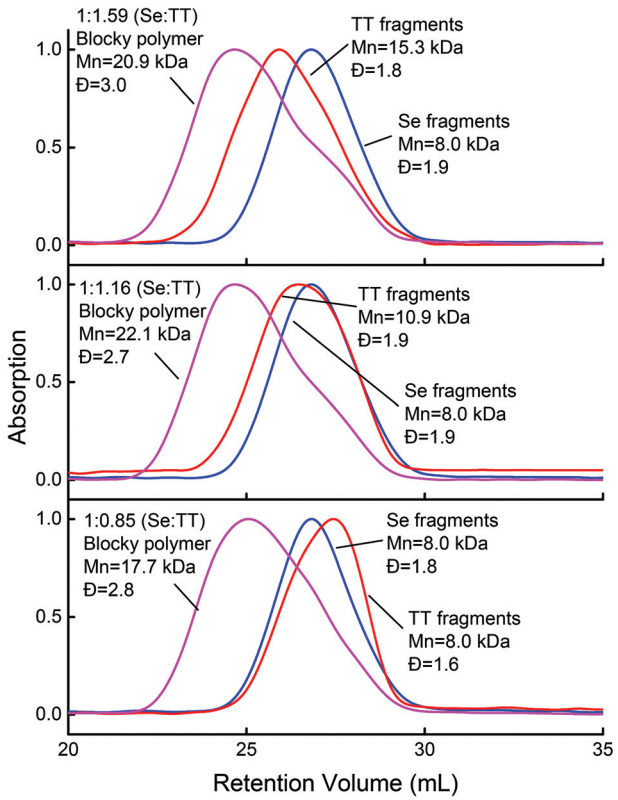

Fig. 1 GPC elution profiles of blocky copolymers (magenta) and their PBDTSe-T (blue) and PBDTTT-C-T fragment reactants (red).

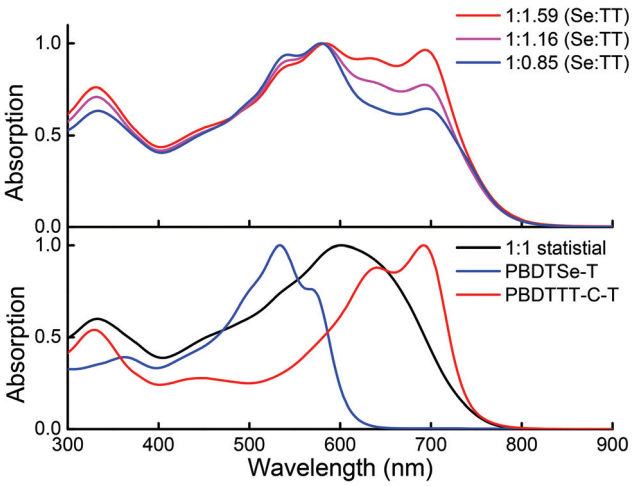

Fig. 2 Normalized absorption spectra of blocky (above), statistical and parent (below) co-polymers in chloroform.

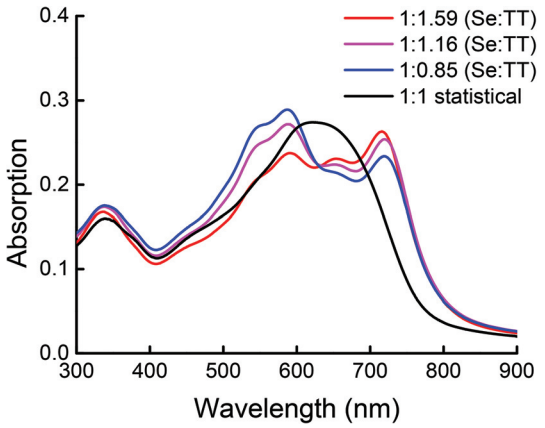

Fig. 3 Absorption spectra of blocky and statistical polymer films spin-coated from chloroform solutions.

Morphology characterization

To further study the solid state morphology of blocky polymers, atomic force microscopy (AFM) images of polymer:$PC_{71}BM$ blend films were collected by both tapping mode and peak force quantitative nanomechanical (PF QEM) mode. In tapping mode phase images (Fig. 4), fiber-like features can be observed for 1 : 1.59 and 1 : 1.16 blocky polymer:$PC_{71}BM$ films, in contrast with their physical mixture analogues that have feature-less phase images. On the other hand structures that

appear in the phase image of 1 : 0.85 blocky polymer:$PC_{71}BM$ film are more aggregated and less ordered, similar to that of the 1 : 0.85 physical mixture: $PC_{71}BM$ film which may due to their higher PBDTSe-T fragment ratios. Peak force quantitative nanomechanical mode AFM allows one to map the adhesion force between the sample and the AFM tip. This depends on the chemical composition of the sample area and is less affected by surface topology. All the three blocky polymer:$PC_{71}BM$ films are networks composed of long and straight fibers (Fig. 5). This is in contrast to the more randomly packed networks of parent polymer:$PC_{71}BM$ films (Fig. S9†) or the disordered short features observed in the statistical polymer or physical mixture films (Fig. S9 and S10†). A clear correlation is observed between the network structure in adhesion mapping and domain morphology in high resolution height images, where adhesion forces are smaller in the core of aggregate domains, and stronger at the edges. Therefore, these networks are most likely composed by soft amorphous polymers where PCBM molecules are embedded within, surrounding the aligned polymer crystallines that appear as aggregated domains in height images.

Solar cell performance

OPV devices were constructed with an inverted structure of ITO/ZnO/Polymer:$PC_{71}BM$/MoO_3/Ag. Device performances are summarized in Table 2. Solar cell devices made using the blocky polymers have similar open circuit voltage (V_{OC}) values of ~0.73 V. These values are in the middle of the V_{OC} of two parent polymers, PBDTTT-C-T (0.77 V) and PBDTSe-T (0.68 V), but lower than V_{OC} of statistical polymer (0.76 V). Fill factors (FF) of both blocky and statistical polymer devices are around 60%, which is in contrast with the relatively low fill factor of PBDTSe-T polymer devices. The values of short circuit current densities (J_{SC}) were statistically the same for the 1 : 1.59, 1 : 1.16 and 1 : 1.85 blocky polymer, despite their different absorption properties. As such, similar power conversion efficiencies (PCEs) were obtained from different blocky polymers. External quantum efficiency (EQE) spectra (Fig. 6) show the similar photon response range of the blocky polymers and PBDTTT-C-T. However the lower V_{OC} leads a lower PCE value.

To further investigate the photovoltaic properties of blocky polymers, we also fabricated devices utilizing physical mixtures of the two parent polymers. The ratios of selenophene and thienothiophene monomers in the physical mixtures are 1 : 1.59, 1 : 1.16 and 1 : 0.85, corresponding to the ratios of selenophene and thienothiophene monomers in the three blocky analogues. Devices utilizing physical mixtures have the same V_{OC} values as blocky polymer devices. However, increasing the amount of PBDTTT-C-T polymer in the physical mixture from 1 : 0.85 to 1 : 1.59 increases the J_{SC} from 13.7 ± 0.2 mA cm^{-2} to

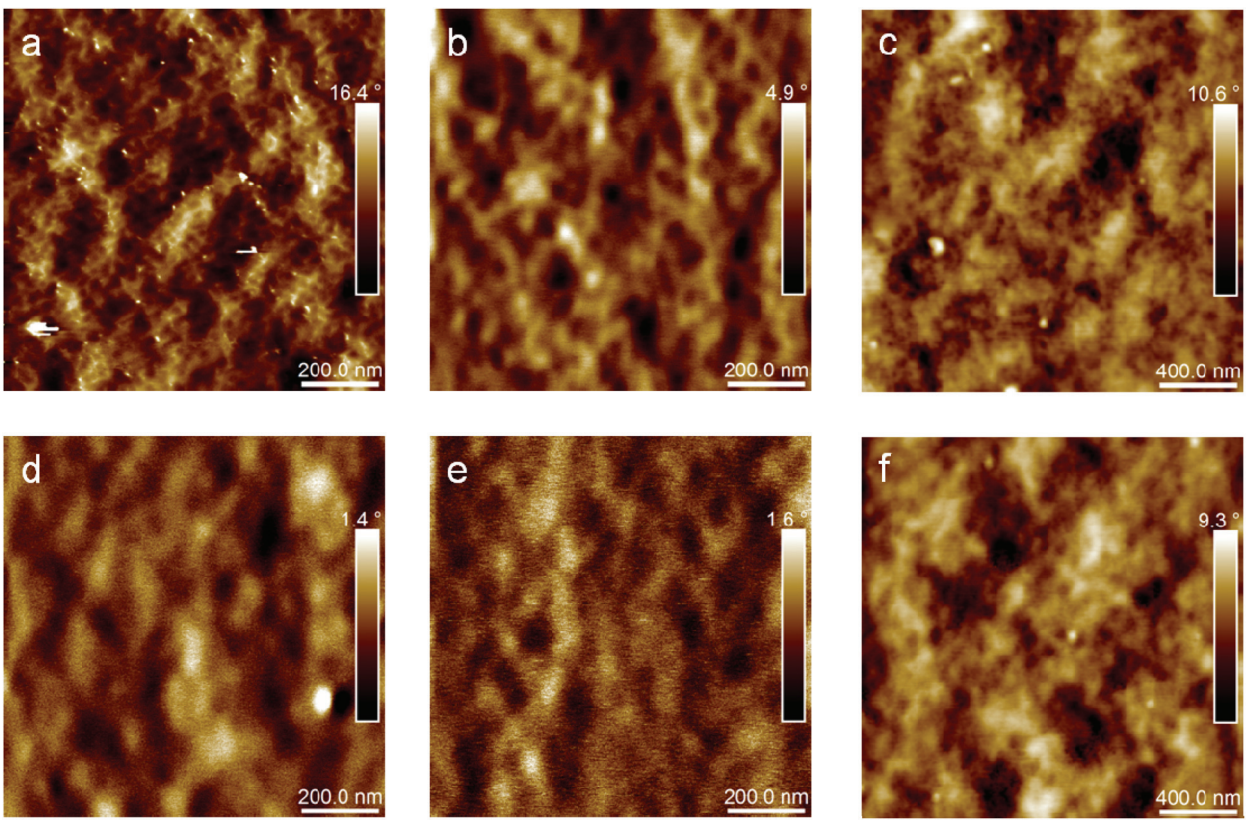

Fig. 4 AFM phase images of 1 : 1.59 blocky (a), 1 : 1.16 blocky (b), 1 : 0.85 blocky (c), 1 : 1.59 physical mixture (d), 1 : 1.16 physical mixture (e) and 1 : 0.85 physical mixture (f) polymer:$PC_{71}BM$ blend films.

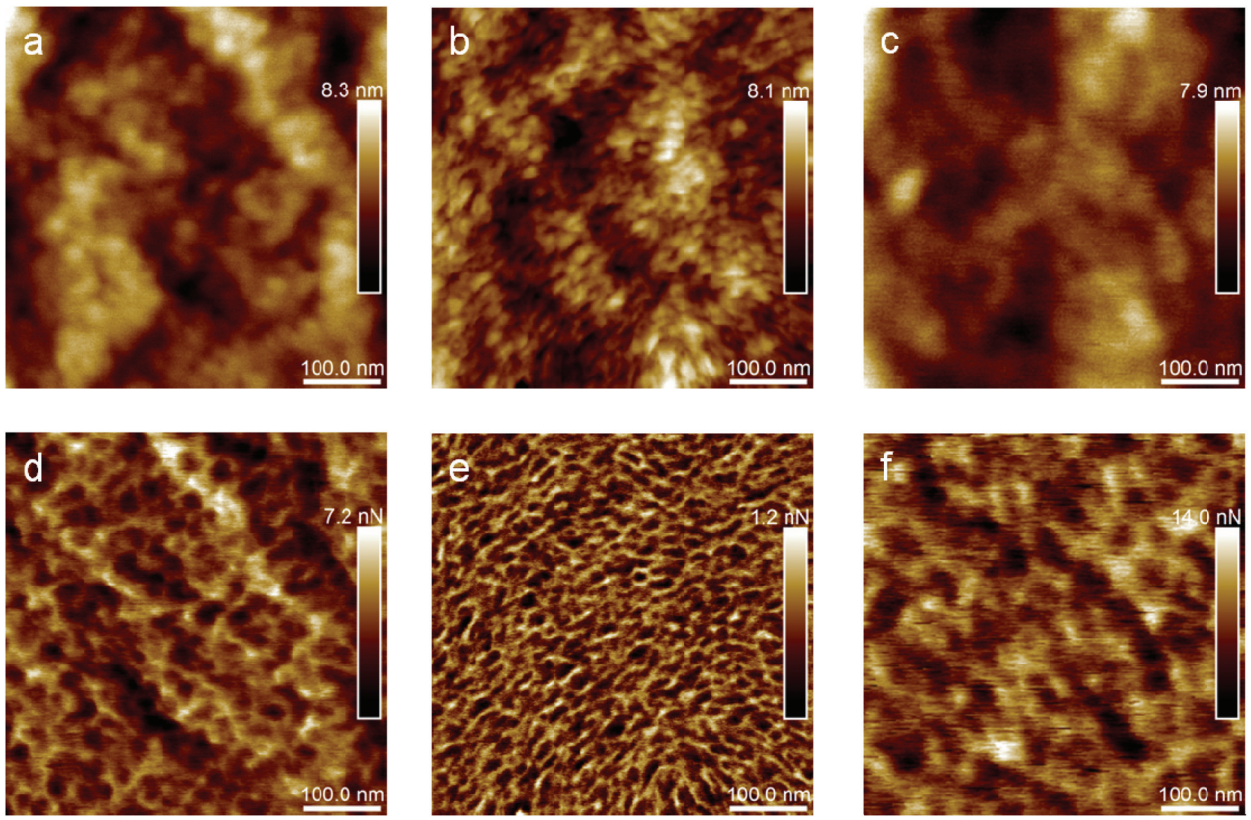

Fig. 5 AFM height (above) and adhesion (below) images of 1 : 1.59 blocky (a, d), 1 : 1.16 blocky (b, e) and 1 : 0.85 blocky(c, f) polymer:$PC_{71}BM$ blend films.

Table 2 Device characteristics of blocky copolymers and physical mixtures. Se : TT (mol : mol) stands for the ratio of the amount of selenophene monomers to the amount of thienothiophene monomers. The standard deviations (SD) are obtained from seven individual devices

Polymer	Se : TT (mol : mol)	J_{SC} (mA cm^{-2})	SD	V_{OC} (V)	SD	FF (%)	SD	PCE (%)	SD
1 : 1.59 blocky	1 : 1.59	13.2	0.2	0.73		60.0	0.6	5.8	0.1
1 : 1.16 blocky	1 : 1.16	13.4	0.3	0.72	0.01	60	2	5.8	0.3
1 : 0.85 blocky	1 : 0.85	13.3	0.2	0.73		58	1	5.6	0.2
Physical mixture	1 : 1.59	14.5	0.2	0.73		64	1	6.8	0.2
	1 : 1.16	14.3	0.4	0.73		63	2	6.6	0.3
	1 : 0.85	13.7	0.2	0.73		64	1	6.4	0.2
1 : 1 Statistical	1 : 1	12.0	0.4	0.76		60.0	0.4	5.4	0.3
PBDTSe-T	1 : 0	8.8	0.5	0.68	0.01	48	3	2.9	0.2
PBDTTT-C-T	0 : 1	14.1	0.4	0.77		61.2	0.9	6.6	0.3

14.5 ± 0.2 mA cm^{-2}, which is in contrast with the consistent J_{SC} values of blocky polymer devices. Mixture devices also have maximum EQE at ~500 nm (Fig. S2†), similar to blocky devices. At wavelengths beyond 700 nm, where neither PBDTSe-T nor $PC_{71}BM$ absorb light, the EQE of the physical mixture devices decreases when the amount of PBDTTT-C-T is reduced. This behavior is different than that of blocky polymers, where the EQE at longer wavelength is nearly identical. The FF of physical mixture devices increases to 63–64%, which is higher than the FF of devices utilizing either the blocky or the two parent polymers. As a result better power conversion efficiencies are observed by mixture devices, while devices incorporating 1 : 1.59 (mol : mol) PBDTSe-T–PBDTTT-C-T mixture exhibited efficiency of 6.8 ± 0.2%. This is even higher than the efficiency of 6.6 ± 0.3% for device utilizing only PBDTTT-C-T polymer. The improved FF may come from more efficient charge dissociation or better charge transport in polymer:PCBM blend.

Measuring photocurrent (J_{ph}) as a function of applied voltage can show the field-dependent charge dissociation in solar cell devices (Fig. 7).[26,27] At low applied voltage ($V_0 - V$), devices utilizing PBDTSe-T polymer, PBDTTT-C-T polymer and

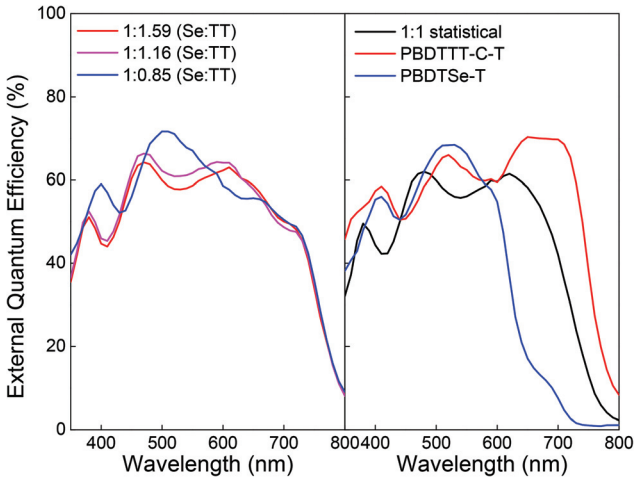

Fig. 6 External quantum efficiency (EQE) spectra of devices of blocky (left), statistical and parent (right) polymers.

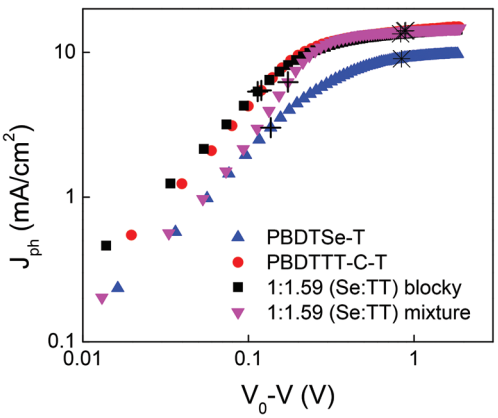

Fig. 7 Photocurrent *versus* applied voltage for devices of PBDTSe-T, PBDTTT-C-T, 1 : 1.59 blocky polymer and 1 : 1.59 physical mixture. The open circuit ($V = V_{OC}$) and short circuit ($V = 0$) points are marked as stars and crosses, respectively.

1 : 1.59 blocky polymer have photocurrents that increase linearly with effective voltage, which is due to the direct correlation between the constant diffusion and drift current.[26] The photocurrents of the blocky polymers were nearly identical to that of PBDTTT-C-T, indicating similar charge generation rate and dissociation efficiency of bound electron–hole pair. On the other hand the effective photocurrent of physical polymer mixtures was the same as PBDTSe-T at lower applied voltage ($V_0 - V < 0.1$ V). Higher applied voltage increases the charge generation, and the photocurrent saturated at a similar voltage as the blocky polymer. This behavior shows a lower charge carrier dissociation efficiency in the physical mixture devices, which need stronger electric field to dissociate bound electron–hole pairs at the donor–acceptor interface. Therefore the higher FF of mixture device is most likely from improved charge transport or reduced bimolecular recombination, both of which result from the formation of separated PBDTSe-T phases in the mixed film. This facilitate more efficient charge extraction with energy levels cascades.[28,29] On the other hand, the different charge dissociation efficiency between blocky and physical mixture cells, and the similarity of their chemical components indicates PBDTSe-T fragments in the blocky polymers do not form separated phases.

Summary

We report here a straightforward synthetic route to blocky D–A copolymers consisting selenophene, benzodithiophene, and thienothiophene. This approach can be applied to many other polymerization methods to prepare many new types of blocky D–A polymers. The blocky polymer structure preserves the optical properties of their respective two-component systems. In this case, the different morphology and photovoltaic behaviors of blocky polymers to their analogous physical mixtures indicates PBDTSe-T fragments in the blocky polymers do not form separated phases, but form crystalline regions containing both fragments. Though more ordered morphologies are observed with blocky polymers, the physical mixture of parent polymers perform better in solar cell devices, which is not well corresponded to the AFM images of blend film surfaces. The polymer crystallinity can be further modified by changing lengths of different blocks. As such, blocky copolymers could be a new tool for tuning the polymer crystallinity, and eventually achieving controllable solid-state morphology for organic electronic applications.

Experimental section

General considerations

Selenophene and $Pd(PPh_3)_4$ were purchased from Sigma-Aldrich. P(4-(5-(2-ethylhexyl)thiophen-2-yl)-8-(5-(octan-3-yl)-thiophen-2-yl)benzo[1,2-*b*:4,5-*b*′]dithiophene-2,6-diyl)bis(trimethylstannane), 1-(4,6-dibromothieno[3,4-*b*]thiophen-2-yl)-2-ethylhexan-1-one units were purchased from Solarmer Materials Inc. All reagents were used as received. Polymer molecular weights were determined with a Viscotek HT-GPC in 1,2,4-trichlorobenzene at 140 °C (1 mL min^{-1} flow rate), using Tosoh Bioscience LLC TSK-GEL GMHHR-HT mixed-bed columns and narrow molecular weight distribution polystyrene standards. NMR spectra were recorded on a Varian Mercury 400 spectrometer operating at 400 MHz ^1H chemical shifts are referenced to the residual protonated chloroform peak at 7.26 ppm. Absorption spectra were recorded on a Varian Cary 5000 UV-vis-NIR spectrophotometer. Powder X-ray diffraction spectra were recorded on a Rigaku MiniFlex 600 X-ray diffractometer.

Polymer synthesis

2,5-Dibromoselenophene: 1.55 g selenophene was dissolved in 10 mL DMF then purged with Ar for 15 min. After purging 4.21 g NBS was added into the solution in four portions within

30 min, then stirred at room temperature for 16 h under argon The reaction mixture was poured into ice water and the product was collected in DCM, washed with brine and water, and then dried with $MgSO_4$. After passing through a plug of silica (chloroform) the final product was isolated as a light yellow oil (2.77 g). ^{1}H NMR (400 MHz, Chloroform-*d*) is identical to that reported in the literature.[30]

Poly[4,8-bis(5-(2-ethylhexyl)thiophen-2-yl)benzo[1,2-*b*:4,5-*b*′]-dithiophene-2,6-diyl-*alt*-selenophene]: bis(trimethylstannane) BDT monomer 271.8 mg and 2,5-dibromoselenophene 86.6 mg were weighed into a dry 25 mL 3-neck flask with 8 mL toluene and 2 mL DMF. After purging with argon for 20 min ~ 13.5 mg of $Pd(PPh_3)_4$ was added, followed by further purging for 20 min. The reaction mixture was stirred and heated to reflux for 20 h under argon. The reaction mixture was then cooled to room temperature, precipitated in 50 mL methanol and filtered through a Soxhlet thimble. The precipitate was extracted with methanol, hexanes and chloroform. The product was recovered from the chloroform fraction and then purified by passing through a plug of silica (chloroform), followed by removal of the solvent under reduced pressure. Yield: 137.0 mg (64.7%). GPC: M_n = 16.3 kDa, M_w = 54.7 kDa, $Đ$ = 3.4.

Poly[4,8-bis(5-(2-ethylhexyl)thiophen-2-yl)benzo[1,2-*b*:4,5-*b*′]-dithiophene-2,6-diyl-*alt*-(4-(2-ethylhexanoyl)-thieno[3,4-*b*]thiophene-)-2-6-diyl)]: The same procedure to the above with 416.7 mg bis(trimethylstannane) BDT monomer and 195.3 mg dibromo thienothiophene monomer was used. Yield: 342.4 mg (88.4%). GPC: M_n = 38.0 kDa, M_w = 88.9 kDa, $Đ$ = 2.3.

{Poly[4,8-bis(5-(2-ethylhexyl)thiophen-2-yl)benzo[1,2-*b*:4,5-*b*′]-dithiophene-2,6-diyl-*alt*-selenophene]}-*stat*-{Poly[4,8-bis(5-(2-ethylhexyl)thiophen-2-yl)benzo[1,2-*b*:4,5-*b*′]dithiophene-2,6-diyl-*alt*-(4-(2-ethylhexanoyl)-thieno[3,4-*b*]thiophene-)-2-6-diyl)]}: The same procedure to the above with bis(trimethylstannane) BDT 303.2 mg, dibromoselenophene 48.4 mg and dibromo TT 71.1 mg was used. Yield: 132 mg (51%). GPC: M_n = 19.2 kDa, M_w = 42.8 kDa, $Đ$ = 2.2.

Bis(trimethylstannane){poly[4,8-bis(5-(2-ethylhexyl)thiophen-2-yl)benzo[1,2-*b*:4,5-*b*′]dithiophene-2,6-diyl-*alt*-selenophene]}: The same procedure to the above with a bis(trimethylstannane) BDT 357.2 mg (411.9 mg for batch 2) and dibromoselenophene 95.0 mg (109.5 mg for batch 2) was used with a reduced refluxing time of 4 h. The reaction mixture was precipitated in hexane, and washed twice with hexane.

Batch 1: Yield 108.7 mg (47%). GPC: M_n = 8.0 kDa, M_w = 14.7 kDa, $Đ$ = 1.8.

Batch 2: Yield 130.7 mg (67%). GPC: M_n = 8.0 kDa, M_w = 15.1 kDa, $Đ$ = 1.9.

Dibromo{ Poly[4,8-bis(5-(2-ethylhexyl)thiophen-2-yl)benzo-[1,2-*b*:4,5-*b*′]dithiophene-2,6-diyl-*alt*-(4-(2-ethylhexanoyl)-thieno-[3,4-*b*]thiophene-)-2-6-diyl)]}: An analogous procedure to the above with 1 : 1.1, 1 : 1.15 or 1 : 1.2 bis(trimethylstannane) BDT : dibromo TT monomer ratios was used. The reaction mixture was precipitated in methanol, and then extracted with hexane and chloroform in a Soxhlet apparatus. Yield 55%–94.0%.

{Poly[4,8-bis(5-(2-ethylhexyl)thiophen-2-yl)benzo[1,2-*b*:4,5-*b*′]-dithiophene-2,6-diyl-*alt*-selenophene]}-*blocky*-{poly[4,8-bis(5-(2-ethylhexyl)thiophen-2-yl)benzo[1,2-*b*:4,5-*b*′]dithiophene-2,6-diyl-*alt*-(4-(2-ethylhexanoyl)-thieno[3,4-*b*]thiophene-)-2-6-diyl)]}: An analogous procedure to the above with a ~1 : 1 bis(trimethylstannane) PBDTSe-T : dibromo PBDTTT-C-T mole ratio was used. The amount of PBDTSe-T and PBDTTT-C-T fragments were estimated based on their M_n.

1 : 1.59 blocky: Yield: 68.5 mg (67%). GPC: M_n = 20.9 kDa, M_w = 61.7 kDa, $Đ$ = 3.0.

1 : 1.16 blocky: Yield: 63.0 mg (68%). GPC: M_n = 22.1 kDa, M_w = 60.0 kDa, $Đ$ = 2.7.

1 : 0.85 blocky: Yield: 135.6 mg (71%). GPC: M_n = 17.7 kDa, M_w = 49.3 kDa, $Đ$ = 2.2.

Solar cell device fabrication and testing

Phenyl-C71-butyric acid methyl ester ($PC_{71}BM$) (American Dye Source) was purchased and used as received. ZnO precursor solution was prepared based on literature procedures.[31] Devices were fabricated on commercial indium tin oxide (ITO) (Thin Film Devices) substrates. These substrates were cleaned in aqueous detergent, deionized (DI) water, acetone, and methanol, and subsequently treated in an air-plasma cleaner for 5 min. ZnO precursor solution was coated onto the substrates at 3000 rpm and annealed at 130 °C in air for 1 h. The final thickness of ZnO was ~40 nm. The substrate was then transferred into a nitrogen-filled glove box, where polymer:$PC_{71}BM$ (1 : 1.5 wt : wt) films were spin-coated at 500 rpm from 1,2-dichlorobenzene solutions with 2 vol.% DIO as an additive. Solutions were stirred at 50 °C overnight and cooled down to room temperature before spin-coating. To finish the device, a 1 nm MoO_3 layer and 80 nm Ag electrode were thermally deposited through a shadow mask at ~10^{-6} torr using an Angstrom Engineering Covap II. All device areas were 0.07 cm^2 as defined by the area of the circular Al cathode. *J–V* characteristics were measured using a Keithley 2400 source meter under simulated AM 1.5 G conditions. The mismatch of the simulator spectrum was calibrated using a Si diode with a KG-5 filter. EQE spectra were recorded and compared with a Si reference cell traceable to the National Institute of Standards and Technology (NIST). AFM scanning was carried directly on solar cell device samples using Bruker Dimension Icon atom force microscope. XRD samples of neat polymer films were drop-coated on Si wafers with thickness of 100–300 nm. XRD samples of polymer:$PC_{71}BM$ blend films were spin-coated on glass substrates using the same procedure as solar cell devices.

References

1 N. Blouin, A. Michaud and M. Leclerc, *Adv. Mater.*, 2007, **19**, 2295–2300.
2 J. Peet, J. Y. Kim, N. E. Coates, W. L. Ma, D. Moses, A. J. Heeger and G. C. Bazan, *Nat. Mater.*, 2007, **6**, 497–500.
3 Y. Liang, Z. Xu, J. Xia, S.-T. Tsai, Y. Wu, G. Li, C. Ray and L. Yu, *Adv. Mater.*, 2010, **22**, E135–E138.

4 S. H. Park, A. Roy, S. Beaupre, S. Cho, N. Coates, J. S. Moon, D. Moses, M. Leclerc, K. Lee and A. J. Heeger, *Nat. Photonics*, 2009, **3**, 297–302.
5 J. Liu, S. Shao, G. Fang, B. Meng, Z. Xie and L. Wang, *Adv. Mater.*, 2012, **24**, 2774–2779.
6 J. Liu, Q. Liang, H. Wang, M. Li, Y. Han, Z. Xie and L. Wang, *J. Phys. Chem. C*, 2014, **118**, 4585–4595.
7 Z. He, C. Zhong, S. Su, M. Xu, H. Wu and Y. Cao, *Nat. Photonics*, 2012, **6**, 591–595.
8 S. Shoaee, S. Subramaniyan, H. Xin, C. Keiderling, P. S. Tuladhar, F. Jamieson, S. A. Jenekhe and J. R. Durrant, *Adv. Funct. Mater.*, 2013, **23**, 3286–3298.
9 D. Gao, B. Djukic, W. Shi, C. R. Bridges, L. M. Kozycz and D. S. Seferos, *ACS Appl. Mater. Interfaces*, 2013, **5**, 8038–8043.
10 X. Guo, M. Zhang, W. Ma, L. Ye, S. Zhang, S. Liu, H. Ade, F. Huang and J. Hou, *Adv. Mater.*, 2014, **26**, 4043–4049.
11 W. C. Tsoi, D. T. James, E. B. Domingo, J. S. Kim, M. Al-Hashimi, C. E. Murphy, N. Stingelin, M. Heeney and J.-S. Kim, *ACS Nano*, 2012, **6**, 9646–9656.
12 D. Muhlbacher, M. Scharber, M. Morana, Z. Zhu, D. Waller, R. Gaudiana and C. Brabec, *Adv. Mater.*, 2006, **18**, 2884–2889.
13 A. M. Ballantyne, L. C. Chen, J. Nelson, D. D. C. Bradley, Y. Astuti, A. Maurano, C. G. Shuttle, J. R. Durrant, M. Heeney, W. Duffy and I. McCulloch, *Adv. Mater.*, 2007, **19**, 4544–4547.
14 J. S. Kim, Z. Fei, S. Wood, D. T. James, M. Sim, K. Cho, M. J. Heeney and J.-S. Kim, *Adv. Energy Mater.*, 2014, **4**, 1400527.
15 H.-Y. Chen, J. Hou, A. E. Hayden, H. Yang, K. N. Houk and Y. Yang, *Adv. Mater.*, 2010, **22**, 371–375.
16 H. Yan, J. Hollinger, C. R. Bridges, G. R. McKeown, T. Al-Faouri and D. S. Seferos, *Chem. Mater.*, 2014, **26**, 4605–4611.
17 A. A. Pollit, C. R. Bridges and D. S. Seferos, *Macromol. Rapid Commun.*, 2015, **36**, 65–70.
18 R. C. Mulherin, S. Jung, S. Huettner, K. Johnson, P. Kohn, M. Sommer, S. Allard, U. Scherf and N. C. Greenham, *Nano Lett.*, 2011, **11**, 4846–4851.
19 L. M. Kozycz, D. Gao, A. J. Tilley and D. S. Seferos, *J. Polym. Sci., Part A Polym. Chem.*, 2014, **52**, 3337–3345.
20 J. Hollinger and D. S. Seferos, *Macromolecules*, 2014, **47**, 5002–5009.
21 J. Hollinger, D. Gao and D. S. Seferos, *Isr. J. Chem.*, 2014, **54**, 440–453.
22 G. L. Gibson, D. Gao, A. A. Jahnke, J. Sun, A. J. Tilley and D. S. Seferos, *J. Mater. Chem. A*, 2014, **2**, 14468–14480.
23 G. L. Gibson and D. S. Seferos, *Macromol. Chem. Phys.*, 2014, **215**, 811–823.
24 L. Huo, S. Zhang, X. Guo, F. Xu, Y. Li and J. Hou, *Angew. Chem., Int. Ed.*, 2011, **50**, 9697–9702.
25 L. Ye, S. Zhang, W. Zhao, H. Yao and J. Hou, *Chem. Mater.*, 2014, **26**, 3603–3605.
26 P. W. M. Blom, V. D. Mihailetchi, L. J. A. Koster and D. E. Markov, *Adv. Mater.*, 2007, **19**, 1551–1566.
27 M. M. Mandoc, W. Veurman, L. J. A. Koster, B. de Boer and P. W. M. Blom, *Adv. Funct. Mater.*, 2007, **17**, 2167–2173.
28 C. W. Schlenker, V. S. Barlier, S. W. Chin, M. T. Whited, R. E. McAnally, S. R. Forrest and M. E. Thompson, *Chem. Mater.*, 2011, **23**, 4132–4140.
29 B. H. Lessard, J. D. Dang, T. M. Grant, D. Gao, D. S. Seferos and T. P. Bender, *ACS Appl. Mater. Interfaces*, 2014, **6**, 15040–15051.
30 B. Lu, S. Zhen, S. Zhang, J. Xu and G. Zhao, *Polym. Chem.*, 2014, **5**, 4896–4908.
31 Y. Sun, J. H. Seo, C. J. Takacs, J. Seifter and A. J. Heeger, *Adv. Mater.*, 2011, **23**, 1679–1683.

